

Repulsion Between Inorganic Particles Inserted Within Surfactant Bilayers

Doru Constantin,^{1,*} Brigitte Pansu,¹ Marianne Impéror,¹ Patrick Davidson,¹ and François Ribot²

¹Laboratoire de Physique des Solides, Université Paris-Sud, CNRS, UMR8502, 91405 Orsay Cedex, France.

²Laboratoire de Chimie de la Matière Condensée, Université Paris VI, CNRS, UMR7574, 75252 Paris Cedex 05, France.

(Dated: July 13, 2021)

We study by synchrotron small-angle X-ray scattering highly aligned lamellar phases of a zwitterionic surfactant, doped with monodisperse and spherical hydrophobic inorganic particles as a function of particle concentration. Analysis of the structure factor of the two-dimensional fluid formed by the particles in the plane of the bilayer gives access to their membrane-mediated interaction, which is repulsive, with a contact value of about $4 k_B T$ and a range of 14 Å. Systematic application of this technique should lead to a better understanding of the interaction between membrane inclusions.

PACS numbers: 87.16.dt, 61.05.cf, 82.70.Dd

In the last decades, much effort was dedicated to the understanding of self-assembled membranes, and in particular of the interaction between membrane inclusions and the host bilayer. This is a challenging problem, since the membrane must be considered as a many-particle system, its properties being collectively determined by the assembly and not by the chemical properties of the individual molecules [1]. Notwithstanding the complexity of the system, the concepts developed in soft matter physics should be operative in this context and even ‘simplified’ models could yield valuable information. For this reason, a considerable body of work deals with the theoretical modelling and numerical simulation of such mixed systems, aiming in particular to determine the membrane-mediated interaction between inclusions [2]. Thorough understanding of these interactions could make a substantial contribution to topics as diverse as the formulation of new composite systems and understanding the activity of membrane proteins.

However, this theoretical work was not yet matched by enough experimental results. The first such data was obtained by directly measuring the radial distribution function of membrane inclusions using freeze-fracture electron microscopy (FFEM) [3]. These data were compared to liquid state models and could be described by a hard-core model with, in some cases, an additional repulsive or attractive interaction [4]. FFEM was not extensively used, undoubtedly due to the inherent experimental difficulties; moreover, it is not obvious that the distribution measured in the frozen sample is identical to that at thermal equilibrium.

Considering the typical length scales to be probed, X-ray and neutron scattering techniques [5] are uniquely adapted to the study of this problem. As an example, the pores formed by the antimicrobial peptide alamethicin in dimyristoylphosphatidylcholine bilayers were shown to repel each other [6]. These studies are however hindered by the low scattering contrast of the proteins (and, in many cases, by their scarcity), whence the practical (and also the fundamental) interest of finding out whether other –perhaps more adapted– particles can be inserted within membranes.

The purpose of this Letter is to show that self-assembled bilayers can be doped with significant amounts of (hydropho-

bic and charge-neutral) hybrid nano-objects and that these probes can be used to determine accurately the membrane-mediated interaction. Their use presents substantial advantages: they are “rigid” (fixed atomic configuration) and perfectly monodisperse, therefore imposing a well-defined membrane deformation, whereas membrane proteins can assume various conformations; their scattering contrast is high (due to the presence of metal atoms); their surface properties can be tailored by changing the nature of the grafted ligands. Conceptually, these inclusions are also easier to model, since they do not “break” the surface of the monolayer and hence there is no contact line, where the choice of the boundary condition would be somewhat delicate [7].

This approach can help clarify long-standing questions, such as: Is a continuous model sufficient for an accurate description of the membrane and, if so, down to what length scale? What are the relevant parameters and how can they be measured? What are the specificities of mixed bilayers, and in particular of lipid membranes (microscale separation, raft formation etc.)? In the long run, systematic studies should yield a clearer picture of membranes as two-dimensional complex systems.

The nanoparticles used here are butyltin oxo clusters $\{(\text{BuSn})_{12}\text{O}_{14}(\text{OH})_6\}^{2+}(4\text{-CH}_3\text{C}_6\text{H}_4\text{SO}_3^-)_2$, denoted by BuSn12 in the following. They were synthesized and characterized as described in reference [8] (for their structure, see Figure 1 in this reference). They were dissolved in ethanol at a concentration of 23.47 wt.%.

The zwitterionic surfactant, dimethyldodecylamine-N-oxide (DDAO) was purchased from Sigma-Aldrich and dried in vacuum (using a liquid nitrogen-cooled solvent trap) for 20 h. No weight loss was observed after this step, so we conclude that the surfactant was dry as supplied (see [9] for a detailed discussion). DDAO was then dissolved in isopropanol at a concentration of 23.02 wt.%.

We mixed the BuSn12 and DDAO solutions to yield the desired particle concentrations, and then dried the mixtures in vacuum; the final (dry) mass was about 200 mg for each sample. We then added water at a concentration of 15–27 wt.% of the final hydrated mixtures, which are thus in the fluid lamellar L_α phase (see the phase diagram of the undoped system

in [9]). The molecular weight of DDAO is 229.40 (Sigma-Aldrich), its density is 0.84g/cm^3 and the thickness of the bilayer is $25 \pm 1\text{\AA}$ [10], yielding an area per surfactant molecule $A_{\text{DDAO}} = 37.8\text{\AA}^2$. For the BuSn12 particles, we take a molecular weight of 2866.7 and a density of 1.93g/cm^3 [8]. Using these values and neglecting the increase in bilayer surface due to the inserted particles yields the (two-dimensional) number density of particles in the plane of the membrane, n .

The samples were prepared in flat glass capillaries (Vitro-Com Inc., Mt. Lks, N.J.), $100\ \mu\text{m}$ thick and $2\ \text{mm}$ wide by gently sucking in the lamellar phase using a syringe. The capillaries were flame-sealed. Good homeotropic alignment (lamellae parallel to the flat faces of the capillary) was obtained by thermal treatment, using a Mettler FP52 heating stage. The samples were heated into the isotropic phase (at $130\text{ }^\circ\text{C}$) and then cooled down to the lamellar phase at a rate of $1\text{ }^\circ\text{C/min}$.

The small-angle x-ray scattering measurements were performed at the European Synchrotron Radiation Facility (ESRF, Grenoble, France) on the bending magnet beamline BM02 (D2AM), at a photon energy of $11\ \text{keV}$. See reference [11] for more details on the setup. The data was acquired using a CCD Peltier-cooled camera (SCX90-1300, from Princeton Instruments Inc., New Jersey, USA) with a resolution of 1340×1300 pixels. Data preprocessing (dark current subtraction, flat field correction, radial regrouping and normalization) was performed using the `bm2img` software developed at the beamline.

The incident beam was perpendicular to the flat face of the capillary (parallel to the smectic director, which we take along the z axis.) Thus, the scattering vector \mathbf{q} is mostly contained in the (x, y) plane of the layers, and the measured scattered signal $I(\mathbf{q})$ probes inhomogeneities of the electron density in this plane. Since the bilayers form a two-dimensional liquid, the scattering pattern exhibits azimuthal symmetry: $I = I(q = |\mathbf{q}|)$. We also measured the scattering intensity of two BuSn12/ethanol solutions in the same type of capillary. The accessible scattering range was $0.04 < q < 0.9\text{\AA}^{-1}$. Since the electron density of the butyl chains is similar to that of the dodecyl chains within the bilayers and to that of ethanol, we expect the electron contrast of the particles to be due exclusively to their inorganic core, which is slightly ovoidal, with an average radius of $4.5\ \text{\AA}$. Indeed, the intensity at higher scattering vectors ($q > 0.5\text{\AA}^{-1}$) is well described for all samples by the form factor of a sphere $|Ff(R, q)|^2$, with a radius $R = 4.5 \pm 0.2\text{\AA}$ used as a free fitting parameter. The interaction between particles is described by the structure factor, defined as $S(q) = I(q)/|Ff(R, q)|^2$ [12]. The structure factors thus obtained are shown in Figure 1 for all in-plane concentrations, listed in the caption.

The additional interaction is viewed as a perturbation with respect to the hard core (disk or sphere) model, taken into account via the random phase approximation (RPA) [13]. In this approach, one obtains the direct correlation function of the perturbed system $c(r)$ from that of the reference system

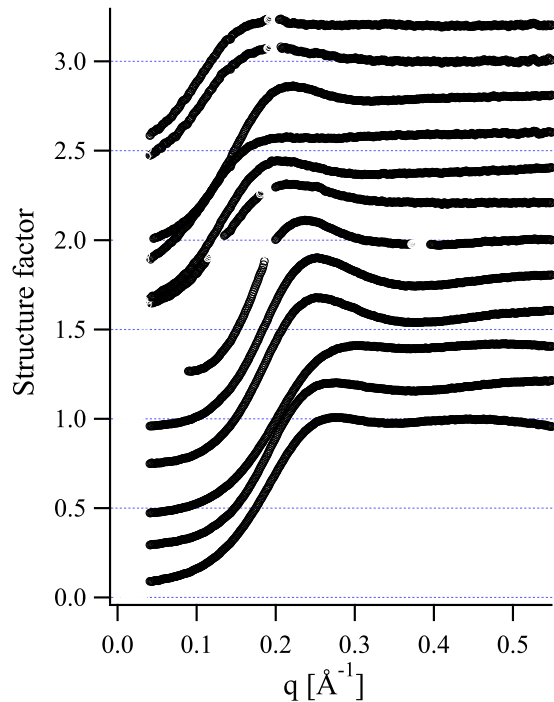


FIG. 1: Structure factors $S(q)$ of the 2D fluid formed by the BuSn12 particles in the plane of the membranes, for different concentrations, from top to bottom: $n = 0.217, 0.231, 0.429, 0.434, 0.451, 0.584, 0.801, 1.102, 1.275, 1.976, 2.147,$ and $2.304 \cdot 10^{-3}\text{\AA}^{-2}$. The curves are shifted vertically in steps of 0.2 . Gaps in the curves correspond to the presence of (weak) lamellar peaks, due to occasional alignment defects, mainly taking the form of oily streaks.

$c_{\text{ref}}(r)$ as: $c(r) = c_{\text{ref}}(r) - \beta U(r)$ [14] or, equivalently:

$$n\beta\tilde{U}(q) = S^{-1}(q) - S_{\text{ref}}^{-1}(q) \quad (1)$$

with $\beta = (k_B T)^{-1}$.

In three dimensions, the reference structure factor S_{ref}^{3D} for BuSn12 particles dissolved in ethanol is given by a hard sphere interaction (in the Percus-Yevick approximation [15, 16]) with a hard-core radius of $4.5\ \text{\AA}$; the numerical particle density n_{3D} (in 3D) is determined from the mass concentration of the solutions.

In two dimensions, an analytical form for the structure factor S_{ref}^{2D} of hard disks was given by Rosenfeld [17]; we use the same core radius of $4.5\ \text{\AA}$ as above. The Fourier transform of the interaction potential, $\tilde{U}(q)$, obtained by applying relation (1) to the data in Fig. 1, is shown in Fig. 2 for all concentrations. For ease of calculation, both in two and three dimensions we model the interaction $U(r)$ by a Gaussian, with amplitude U_0 and range ξ :

$$U(r) = U_0 \exp[-(r/\xi)^2/2] \quad (2)$$

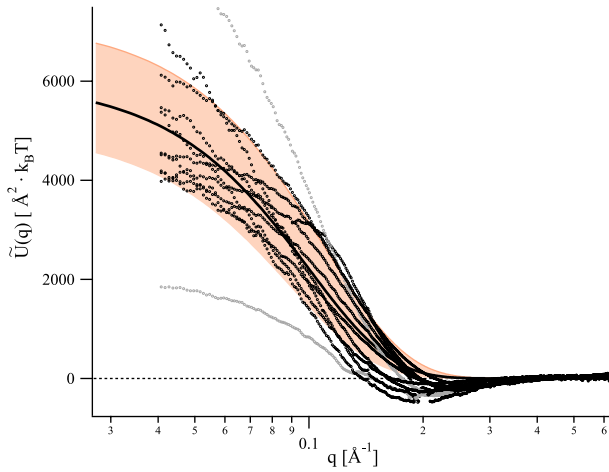


FIG. 2: The Fourier transform of the interaction potential, $\tilde{U}(q)$, (open dots) obtained from the structure factors in Figure 1 in the RPA approximation (1). The solid line is a Gaussian model. The shaded area is chosen to cover most experimental points and is also delimited by two Gaussians (see text for details). The data points far above and far below the shaded range correspond to $n = 0.429$ and $0.584 \cdot 10^{-3} \text{Å}^{-2}$, respectively (third and sixth curve from the top in Figure 1).

with $\tilde{U}(q)$ the Fourier transform of $U(r)$, given by:

$$\tilde{U}(q) = \begin{cases} 2\pi U_0 \xi^2 \exp\left[-(q\xi)^2/2\right] & \text{in 2D} \\ (2\pi)^{3/2} U_0 \xi^3 \exp\left[-(q\xi)^2/2\right] & \text{in 3D} \end{cases} \quad (3)$$

With the exception of two curves (for $n = 0.429$ and $0.584 \cdot 10^{-3} \text{Å}^{-2}$) that are anomalously high or low, respectively, all data points are reasonably well covered by the shaded area in Figure 2, limited by two Gaussians (2D case in Eq. 3), with $U_0 = 3.22 k_B T$ and $\xi = 15.71 \text{Å}$ for the lower bound and $U_0 = 6.93 k_B T$, $\xi = 12.86 \text{Å}$ for the upper bound. The solid line, giving approximately the midline of the shaded area, is described by $U_0 = 4.75 k_B T$ and $\xi = 14.14 \text{Å}$. The apparent negative values of $\tilde{U}(q)$ around $q = 0.2 \text{Å}^{-1}$ in Figure 2 are probably due to the enhancement of the interaction peak of $S(q)$ with respect to the reference potential by the presence of the repulsive interaction; this feature is not captured by the simple RPA treatment. The (real-space) interaction potentials $U(r)$ corresponding to the aforementioned values of U_0 and ξ are plotted in Figure 3, using the same convention. Thus, the solid line is the estimate for the interaction and the shaded area the uncertainty due to the value spread in Figure 2. Of course, for $r < 2R = 9 \text{Å}$ the repulsion is due to the hard core (solid vertical line).

To make sure that the interaction is induced by the membrane, we also show the repulsion measured for BuSn12 particles in ethanol (lower solid line in Figure 3); its amplitude and range are clearly lower than for the interaction in the membrane (for reference, $U_0 = 4 k_B T$ and $\xi = 7 \text{Å}$). It is probably due to the steric repulsion between the butyl chains grafted onto the inorganic core.

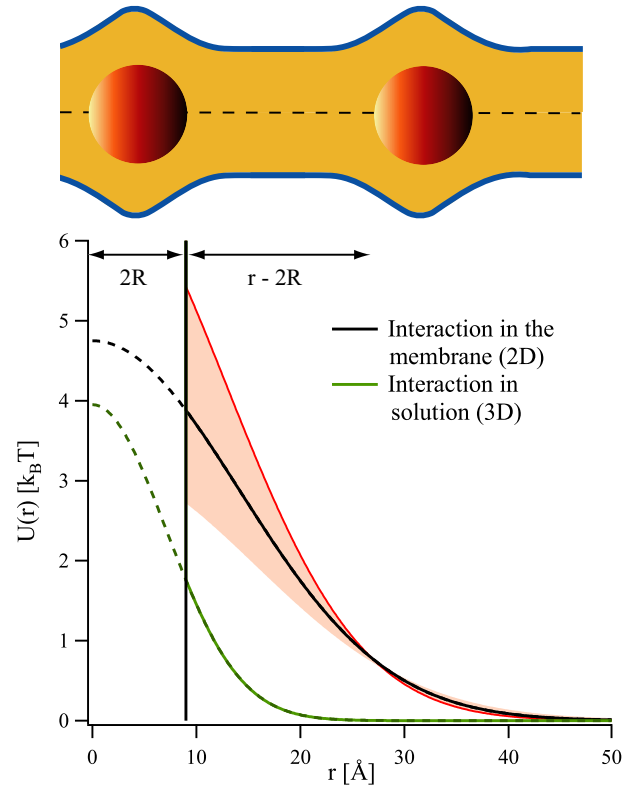


FIG. 3: Interaction potential $U(r)$ of the BuSn12 particles within the bilayers, obtained by taking the inverse Fourier transform of the solid line and the shaded area in Figure 2 (see text for the numerical values). The lower curve is the interaction potential of the particles in ethanol. The solid vertical line marks the hard core interaction with radius 4.5Å

The main result of this work is hence that the (two-dimensional) interaction between BuSn12 particles inserted within DDAO bilayers can be described by a potential of the form (2), with $U_0 = 5 \pm 1 k_B T$ and $\xi = 14 \pm 1 \text{Å}$. Below, we discuss briefly the various theoretical predictions, but a direct comparison cannot be made since they generally concern cylindrical inclusions that traverse the membrane, without being covered by the monolayers.

The simplest approach is to model the membrane as a continuous medium and write the free energy of the bilayer+inclusions system in terms of elastic deformation, described by the Helfrich Hamiltonian [18], where the molecular properties of the bilayer are abstracted into mesoscopic parameters, such as the bending and stretching moduli and the spontaneous curvature of the monolayer. A systematic study was performed in the group of Pincus [19–21]. Their results highlight the importance of the spontaneous curvature of the monolayers c_0 : the interaction is attractive when c_0 vanishes (the elastic energy is minimized by the aggregation of inclusions) but can become repulsive when the deformation induced by the inclusion is such that the curvature of the individual monolayer has the sign of c_0 . In our case, this would mean that the DDAO monolayers tend to have $c_0 > 0$ (convex

head-groups, see the sketch in Figure 3)

However, inclusions also perturb the structure of the membrane by restricting the conformation of the lipid chains in their vicinity [22], and this can lead to significant interaction, even in the absence of “large scale” bilayer deformation (no hydrophobic mismatch.) In particular, Lagüe et al. [23] find that “smooth” hard cylinders repel each other in some lipid bilayers; the amplitude and range of this interaction is in qualitative agreement with our results (for cylinders with a 5 Å radius in dioleoylphosphatidylcholine bilayers, the repulsive lipid-mediated interaction has a maximum value of $7 k_B T$ and extends 20 Å from contact.) Nonetheless, the interaction is highly dependent on the chemical structure of the lipid, so a meaningful comparison is difficult to make using the available data.

Recently, some efforts were made [24, 25] to account for both effects (elastic energy and restrictions on chain conformations) within an extended model, including as variables both the variation in membrane thickness and the local molecular tilt. Their coupling removes the symmetry between the positive and negative spontaneous curvature values, leading to repulsion only for $c_0 > 0$ combined with negative hydrophobic mismatch (bilayer “pinching”.) At first sight this prediction seems to be at odds with our system, but the difference in geometry plays an important role: in our case, we expect the particles to be covered by positively curved monolayer caps (energetically favourable), while the calculation in [25] considers the inclusions as vertical cylinders. A more accurate comparison should be very interesting.

We have shown that nano-objects can be used to probe the properties of self-assembled bilayers; conversely, one can envision using ordered surfactant phases (combining a high degree of order with easy processability and very good wetting properties) to organize and align such objects in view of applications.

The ESRF is gratefully acknowledged for the award of beam time (experiment 02-01-732) and we thank C. Rochas for competent and enthusiastic support. A. Dessombz and A. Poulos are acknowledged for helping with the synchrotron experiments.

* Corresponding author. Tel.: +33 1 69 15 53 94 ; fax: +33 1 69 15 60 86; e-mail address: constantin@lps.u-psud.fr

- [1] M. Ø. Jensen and O. G. Mouritsen, *Biochim. Biophys. Acta-Biomembranes* **1666**, 205 (2004).
 [2] M. M. Sperotto, S. May, and A. Baumgaertner, *Chem. Phys.*

- Lipids* **141**, 2 (2006).
 [3] B. A. Lewis and D. M. Engelman, *J. Mol. Biol.* **166**, 203 (1983); Y. S. Chen and W. L. Hubbell, *Exp. Eye Res* **17**, 517 (1973); R. James and D. Branton, *Biochim. Biophys. Acta* **323**, 378 (1973); J. R. Abney, J. Braun, and J. C. Owicki, *Biophys. J.* **52**, 441 (1987).
 [4] L. T. Pearson, B. A. Lewis, D. M. Engelman, and S. I. Chan, *Biophys. J.* **43**, 167 (1983); L. T. Pearson, J. Edelman, and S. I. Chan, *Biophys. J.* **45**, 863 (1984); J. Braun, J. R. Abney, and J. C. Owicki, *Biophys. J.* **52**, 427 (1987).
 [5] K. He, S. J. Ludtke, H. W. Huang, and D. L. Worcester, *Biochem.* **34**, 15614 (1995); K. He, S. J. Ludtke, D. L. Worcester, and H. W. Huang, *Biophys. J.* **70**, 2659 (1996); L. Yang, T. Weiss, T. Harroun, W. Heller, and H. Huang, *Biophys. J.* **77**, 2648 (1999).
 [6] D. Constantin, G. Brotons, A. Jarre, C. Li, and T. Salditt, *Biophys. J.* **92**, 3978 (2007).
 [7] T. A. Harroun, W. T. Heller, T. M. Weiss, L. Yang, and H. W. Huang, *Biophys. J.* **76**, 3176 (1999).
 [8] C. Eychenne-Baron, F. Ribot, N. Steunou, C. Sanchez, F. Fayon, M. Biesemans, J. C. Martins, and R. Willem, *Organometallics* **19**, 1940 (2000).
 [9] V. Kocherbitov and O. Söderman, *J. Phys. Chem. B* **110**, 13649 (2006).
 [10] G. Orådd, G. Lindblom, G. Arvidson, and K. Gunnarsson, *Biophys. J.* **68**, 547 (1995); P. Wåsterby and P.-O. Quist, *Langmuir* **14**, 3704 (1998).
 [11] J. P. Simon, et al., *J. Appl. Cryst.* **30**, 900 (1997).
 [12] P. M. Chaikin and T. C. Lubensky, *Principles of Condensed Matter Physics* (Cambridge University Press, 1995).
 [13] H. C. Andersen and D. Chandler, *J. Chem. Phys.* **53**, 547 (1970).
 [14] J.-P. Hansen and I. R. McDonald, *Theory of Simple Liquids* (Academic Press, New York, 1986), 2nd ed.
 [15] M. S. Wertheim, *Phys. Rev. Lett.* **10**, 321 (1963).
 [16] E. Thiele, *J. Chem. Phys.* **39**, 474 (1963).
 [17] Y. Rosenfeld, *Phys. Rev. A* **42**, 5978 (1990).
 [18] W. Helfrich, *Z. Naturforsch. C* **28**, 693 (1973).
 [19] N. Dan, P. Pincus, and S. Safran, *Langmuir* **9**, 2768 (1993).
 [20] N. Dan, A. Berman, P. Pincus, and S. Safran, *J. Phys. II France* **4**, 1713 (1994).
 [21] H. Aranda-Espinoza, A. Berman, N. Dan, P. Pincus, and S. Safran, *Biophys. J.* **71**, 648 (1996).
 [22] S. Marčelja, *Biochim. Biophys. Acta* **455**, 1 (1976); D. R. Fattal and A. Ben-Shaul, *Biophys. J.* **65**, 1795 (1993); T. Sintes and A. Baumgärtner, *Biophys. J.* **73**, 2251 (1997); S. May and A. Ben-Shaul, *Phys. Chem. Chem. Phys.* **2**, 4494 (2000).
 [23] P. Lagüe, M. J. Zuckermann, and B. Roux, *Biophys. J.* **79**, 2867 (2000); P. Lagüe, M. J. Zuckermann, and B. Roux, *Biophys. J.* **81**, 276 (2001).
 [24] S. May, *Langmuir* **18**, 6356 (2002).
 [25] K. Bohinc, V. Kralj-Iglič, and S. May, *J. Chem. Phys.* **119**, 7435 (2003).